J. At. Mol. Sci.
doi: 10.4208/jams.072015.082315a

Vol. **6**, No. 3, pp. 206-214
September 2015

Investigating spectral red shift mechanism of fluorescent chromophores using time-dependent density functional theory

Pei li Zhao[a], Huan Lou[a], JingBin Xu[b], and Jian Song[a,*]

[a] *College of Physics and Electronic Engineering, HeNan Normal University, Xin Xiang, 453007, China*
[b] *Mudan Jiang Medical University, Mudan Jiang, 157011, China*

Received 20 July 2015; Accepted (in revised version) 23 August 2015
Published Online 30 September 2015

Abstract. Several fluorescent protein fluorophores with regular substitution were investigated in gas phase using TDDFT with long range corrected functional. Absorption and emission of both neutral and anionic chromophore states were calculated. The spectral shift amplitudes of calculation are in good agreement with experiment. The further intramolecular charge transfer process analysis show that conjugated area, charge transfer number/distance and transfer efficiency can affect spectral shift. Specially, the "N" atom with lone pair electrons of conjugated ring has an important influence on charge transfer process, and the conjugated length between hydroxyl and bridge bond only impact the anionic spectral shift. Our results about fluorescent chromophore spectral red shift mechanism do provide positive clues on new experimental far-red fluorescent protein designing.

PACS: 87.64.kv

Key words: Fluorescent protein; spectral red shift; TDDFT; Intramolecular Charge Transfer.

1 Introduction

Green fluorescent protein (GFP), which was first discovered in the jelly-fish *Aequorea victoria* [1, 2], has been widely adopted as an internal fluorescent label in the field of cellular and molecular biology[3, 4]. GFP is particularly useful for tagging and observing gene expression, protein localization, and cell development [5, 6, 7]. The GFPs possess a barrel-like structure, in which the chromophore locates in the center and links with the surrounding α-helices [2]. The measured optical absorption spectrum of the wild type

*Corresponding author. *Email address:* songjian@htu.cn (J. Song)

(wt) GFP has a strong peak at 395nm and a minor one at 475nm, which have been attributed to the neutral and the negatively charged (anionic) states, respectively [8]. The neutral and anionic chromophores give emission spectral peaks around 503-508 nm [9].

The wild type fluorescent protein (FP) can be engineered into the mutants with the emission frequencies covering the full range of the visible electromagnetic spectrum [10, 11, 12, 13, 14]. These molecules, especially the red fluorescent proteins (RFPs) and far-red fluorescent proteins (f-RFPs) with the emission frequency above 600 nm, provide the powerful tools for biochemical and biomedical research in living cells [15, 16, 17]. A suitable RFP is compatible with the existing confocal and wide-field microscopes and thus increases the capacity to image the entire animal. The far-red fluorescent proteins whose emission maxima reach 650 nm are particularly high demanding for multicolor labeling and whole-mount labeling because long wavelength can penetrate tissue more deeply and easily.

The designing of mutated FPs, however, still mostly depends on experimental researcher's scientific intuition, which significantly retards the discovery of new functional mutants, since the mutagenesis of the FPs is a costing and tedious task. A better understanding of molecular details of the FP fluorescence transitions, by the theoretical modeling, can help rationalize the FP designing and summarize the possible general rules. Additionally, modeling and analyzing the fluorescence mechanism of a series of FP molecules can potentially propose new FP mutants with better performances. To achieve this purpose, however, the modeling techniques adopted should have a balance between the computational cost and the accuracy, since large amount of computation is needed. The multiconfigurational self-consistent field (MCSCF) theory [18] based methods such as CASSCF/CASPT2 [19] can provide accurate descriptions of the small molecular systems. Applications of these methods to the larger systems, however, often encounter problems due to their considerable computational cost.

Another commonly adopted option for the fluorescence frequency calculation is the time-dependent density functional theory (TDDFT) with long-range corrected (LRC) exchange-correlation functional. TDDFT can greatly reduce computational cost compared with the MCSCF techniques. At the same time, LRC functional can deal with the long range electron correlation better, which is common in π-conjugated fluorescent chromophore transition process, than conventional hybrid functional such as B3LYP [20]. Taking Filippi's work for example, LRC functional CAM-B3LYP [21] and LC-BLYP [22] present overall good agreement with the extrapolation of solution experiments to vacuum conditions for wild-type GFP as well as wave function methods [23].

In Wang's fluorescent protein mutant work [24], a new hydroxyquinoline ring was introduced to substitute phenol of the fluorophore in diverse fluorescent proteins and significantly red-shifted excitation and emission spectra were achieved. Inspired by this, here we select and design a series of fluorophores with different substitution as study objects. TDDFT with LRC functional method has been employed to investigate the structure related regularity of fluorescent protein spectral red shift and clarify the underlying

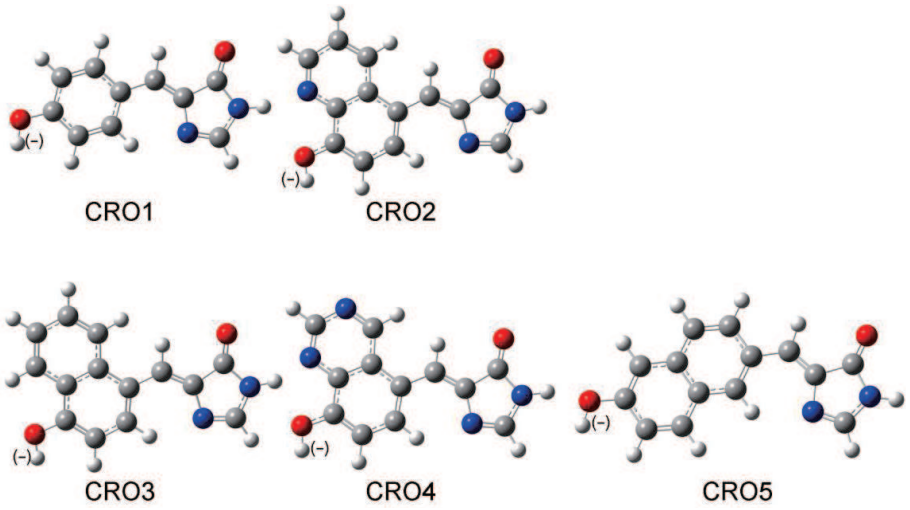

Figure 1: All the five chromophore structure models. The corresponding anionic structures can be obtained by losing a proton in the left hydroxy.

atomic level mechanism. The end goal is try to provide some new theoretical clues and foundations for new far-red fluorescent proteins design. This text is organized as follows: the second part briefly introduces the chromophore structure models and quantum chemistry methods we employed. The calculated results and discussion of fluorophores' absorption and emission and population analysis are in the third section. The conclusions are followed in the end.

2 Models and methods

Five chromophore structure models we employed are displayed in Fig. 1. They have certain laws in conjugated ring structure substitution and are labeled CRO1, CRO2, CRO3, CRO4 and CRO5, respectively. Compared with CRO1, which comes from *Aequorea victoria* GFP, the CRO2 chromophore have a hydroxyquinoline ring displacing the parent phenol ring of CRO1. While the CRO3 and CRO4 chromophores have one hybrid "N" atom reduced and added for hydroxyquinolin ring, respectively. The last CRO5 fluorophore is an isomer of CRO3 but has completely different substitution positions. It is should be noted that CRO2 chromophore comes from *sfGFP-66-HqAla* fluorescent proteins, which are synthesized already by Wang [24], and the last three chromophores are supposed by us. All the chromophore anionic states are formed by losing one proton of hydroxyl in the left conjugated ring.

The ground and excited states geometries of both neutral and anionic chromophore models were optimized using CAM-B3LYP functional with 6-311g (d, p) basis set. The frequency analysis calculations were followed to check configuration stability. Based on stable configurations, then the vertical excited state calculations were carried out using

Table 1: Calculated absorption and emission energies of different chromophore models, and the corresponding oscillator strengths and dipole moments. (The unit of energy is eV, the oscillator strength and dipole moment units are a.u.).

	CRO1		CRO2			
	$E(Osc.)$	$Dip.$	$E(Osc.)$	$Dip.$		
Neutral						
$S_0 \rightarrow S_1$	3.88 (0.74)	7.81	3.53 (0.69)	8.02		
$S_1 \rightarrow S_0$	3.26 (0.66)	8.30	3.04 (0.71)	9.48		
Anionic						
$S_0 \rightarrow S_1$	3.29 (0.97)	12.08	3.13 (0.86)	11.21		
$S_1 \rightarrow S_0$	3.13 (0.91)	11.87	2.86 (0.57)	8.18		
	CRO3		CRO4		CRO5	
	E (Osc.)	Dip.	E (Osc.)	Dip.	E (Osc.)	Dip.
Neutral						
$S_0 \rightarrow S_1$	3.48 (0.67)	7.86	3.55 (0.67)	7.73	3.58 (0.69)	7.88
$S_1 \rightarrow S_0$	3.03 (0.71)	9.52	3.01 (0.68)	9.16	3.11 (0.78)	9.89
Anionic						
$S_0 \rightarrow S_1$	3.11 (0.89)	11.73	3.07 (0.73)	9.74	2.75 (0.98)	14.53
$S_1 \rightarrow S_0$	2.96 (0.86)	11.84	2.57 (0.29)	4.67	2.59 (0.83)	13.14

TDDFT with CAM-B3LYP/6-311g (p, d). And the Mulliken population analysis was performed at the same level.

3 Results and discussion

3.1 Spectra of chromophore models

The vertical absorption and emission energies of the five chromophores in gas phase, including the neutral and anionic states, are presented in Table 1. Although the absolute TDDFT excited energies of each state of chromophores can not be comparable to experimental values as usual (usually overestimate the energy) [23, 25], the calculated spectral energies of all the five chromophores have an obvious regularity. From CRO1 to CRO2, which are two already existed fluorescent protein chromophores, all energies present a distinct red shift. The absorption and emission of neutral state have 0.35 eV and 0.22 eV red shifts, respectively. Those shifts of anionic states are 0.16 eV and 0.27 eV. In experiment, the emission spectra of *sfGFP-66-HqAla* protein showed a 0.15 eV red shift compared with *sfGFP* protein [24]. Thus it can be seen that our calculated shift results here are consistent with experiment very well. With the observation of CRO1 and CRO2 chromophore structures as seen in Fig. 1, only the left phenol ring of HBI was substituted by hydroxyquinoline ring. So it means that the more expanded and bigger

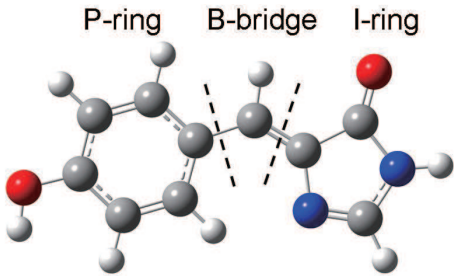

Figure 2: Chromophore decomposition model for Mulliken population, taking CRO1 for example.

conjugated ring seems favor to protein spectral red shift. Another question is whether the hybrid atom (such as "N" atom") or the substitutional postion of ring also can affect the spectral shift. Three modified chromophores, CRO3, CRO4 and CRO5, are displayed in Fig. 1, and their spectral calculation results are showed in Table 1. In chromophore structures of the CRO3 and CRO4, the phenol ring of HBI was substituted by a Naphthol ring and quinoxalinol ring, which reduce and add a "N" atom of hydroxyquinoline ring, respectively. Compared CRO3 with CRO2, the absorption and emission energies have little change except that the emission energy of anionic state of CRO3 blue shift 0.1 eV. While the anionic emission energy of CRO4 chromophore has a 0.29 eV red shift from CRO2. When the substituted position of Naphthol ring was changed, which lead to a longer distance between hydroxyl and the bridge bond as showed in CRO5 of Fig. 1, both the absorption and emission energies appear obvious red shifts. As an isomer, the absorption and emission energies shift about 0.36 $\sim$ 0.37 eV from CRO3 to CRO5.

3.2 Intramolecular charge transfer

To further understand the above spectral shift, intramolecular charge transfer analysis is performed on all the neutral and anionic chromophores in this section. Intramolecular charge transfer process is known as a significant factor that impacts spectra of many conjugated chromophores or polymers [26, 27, 28]. According to quantum chemistry theory, charge transfer often is accompanied long range electron correlation, which can lead to transition energy correction. To explore intramolecular charge transfer of chromophores, first we divide all chromophore structures into three segments. Taking CRO1 chromophore for example, the left phenol ring is labed "P-ring", the bridge ethylene C and H is labeled "B-bridge", the right imidazolinone ring is labeled "I-ring"(as seen in Fig. 2).

Intramolecular Mulliken population changes in different chromophores are shown in Table 2. In the all states of CRO1 chromophore, there is an distinct intramolecular charge transfer process can be found. For example, the "P-ring" acts as electron donor, the "B-bridge" serves as electron acceptor, and the "I-ring" mostly plays the donor role except in the neutral absorption. In the absorption of neutral CRO1, there are about 0.095 electrons transferring from "P-ring" to "B-bridge" and "I-ring". While in the emission of anionic

Table 2: Intramolecular Mulliken population changes in different chromophore models. All the Δ equal to the population difference between excited state and ground state based on each optimized geometries, S_0 or S_1.

	S_0			S_1		
	ΔP	ΔB	ΔI	ΔP	ΔB	ΔI
Neutral						
*CRO*1	0.095	-0.082	-0.013	0.025	-0.058	0.033
*CRO*2	0.087	-0.062	-0.025	0.016	-0.038	0.022
*CRO*3	0.139	-0.079	-0.060	0.066	-0.057	-0.009
*CRO*4	0.045	-0.043	-0.002	-0.019	-0.019	0.038
*CRO*5	0.149	-0.080	-0.069	0.088	-0.064	-0.024
Anionic						
*CRO*1	0.048	-0.081	0.032	0.045	-0.081	0.037
*CRO*2	0.007	-0.063	0.056	-0.092	-0.025	0.117
*CRO*3	0.035	-0.073	0.038	0.030	-0.074	0.045
*CRO*4	-0.038	-0.036	0.073	-0.166	0.007	0.159
*CRO*5	0.080	-0.068	-0.013	0.094	-0.069	-0.025

CRO1, there are about 0.081 electrons transferring from both "P-ring" and "I-ring" to the middle "B-bridge". When the phenol ring is substituted by hydroxyquinoline for CRO2's "P-ring", each segment's roles retain unchanged, but the charge transfer numbers are changed. In general, the electron donor role of "P-ring" is reduced from CRO1 to CRO2, even the "P-ring" translate to an electron acceptor in anionic emission. We also notice that all the charge transfer numbers between three parts are reduced except in anionic emission. It has reasons to think that the spectral red shift from CRO1 to CRO2 more comes from large conjugated area but not charge transfer amplitude. Because the conjugated degree of hydroxyquinoline ring has been doubled compared with phenol ring. In addition, the lone pair electrons of "N" atom in hydroxyquinoline do not involve in the conjugate bonding, so they can play their electron-attracting ability. In result, it can further weaken the "P-ring" ring's donor role and even change it into an acceptor in anionic emission. This interpretation can be further confirmed when the "N" atom of hydroxyquinoline ring was reduced or added in CRO3 and CRO4, respectively. Compared CRO3 with CRO2, the electron donating ability of "P-ring" has been enhanced in all states. In anionic emission state, the charge transfer number is 0.117 and the range of transfer is the whole chromophore (from "I-ring" to "B-bridge" and "P-ring") in CRO2. While it is not only the number are decreased into 0.074 but also the transfer range is halved (the transfer process from either ends does not pass through the "B-bridge") in CRO3. This helps explain why there is a blue shift from CRO2 to CRO3 in anionic emission. On the contrary, the donating ability of "P-ring" has been suppressed obviously when one "N" atom was added in CRO4. The "P-ring" changes into an electron withdrawing actor in all states except the neutral absorption state. In anionic emission, the

charge transfer process of CRO4 has two traits compared with CRO2: One is larger transfer number, another is more higher transfer degree. As shown in Table 2, the electron transfer number of CRO4 is 0.166 (0.117 of CRO2). And all the electrons transfer across the "I-ring" bridge to reach the left "P-ring" in CRO4 but only part of electrons can arrive in "P-ring" in CRO2. This should be the reason why there is a 0.29 eV red shift in anionic emission from CRO2 to CRO4. When the substituted positions of Naphthol ring have been altered from CRO3 to CRO5, the population of neutral states changes slightly and that of anionic states varies evidently. As seen in Table 2, the electron donating role of "P-ring" is enhanced and the intramolecular charge transfer distance has been increased (electron acceptor extends from "B-bridge" to "B-bridge" and "I-ring") for both anionic absorption and emission states of CRO5 compared with CRO3. These are undoubtedly responsible for the spectral red shift from anionic CRO3 to CRO5. The reason of why there is so large different response between neutral states and anionic states after a longer distance between bridge bond and hydroxy of "P-ring" achieved in CRO5, is generally ascribed to the negative charged hydroxyl of Naphthol ring in anionic states. For neutral states, the hydroxyl of Naphthol ring is nothing special in the charge transfer process, so the substitution position change has limited impact on spectra. However in anionic states the hydroxyl, which losses one proton and carries net negative charges, plays an important part in charge transfer. For example, it can provide more free charge and turn into a potential power for electron donation. So when the distance between hydroxyl and "I-ring" is enlarged, it means a longer conjugated distance achieved and results in an enhanced charge transfer process.

4 Conclusions

Systemic fluorescent protein chromophores, which have regular side chain substitutions, have been investigated using TDDFT with long range corrected functional CAM-B3LYP method. In our calculation, experiment comparable shifts have been achieved for already synthesized fluorescent protein chromophore structures. And the results show that long related correction TDDFT can provide reasonable spectral shift trends rather than absolute spectral values. Combined population analysis with calculated absorption and emission values for all the chromophore models, several conclusions about spectral shift structure-property relationship can be arrived:

1) Both longer conjugated area and larger intramolecular charge transfer process can bring out spectral red shift.

2) The charge transfer number, charge transfer distance and the proportion of realized long distance transmission charge number all could influence spectral shift

3) The intramolecular charge transfer direction do have no effect on spectral shift

4) The "N" atom of conjugated ring, which has lone pair electrons, presents power electron attracting ability and can affect the whole intramolecular charge transfer pattern seriously.

5) The distance between hydroxyl and bridge bond has an impact on anionic but not neutral states' charge transfer process.

It is gratifying that all the above conclusions are nicely coherent with quantum chemistry correlated energy theory. The more correlated energy correction (such as larger conjugated range and higher charge transfer process) brings out excited state reduction. It should be noted that if the right imidazolinone ring or the side chain of imidazolinone ring were changed, or the complex protein environments of chromophores were considered, the spectral shift regularity summarized here may be corrected. Those are not discussed in this manuscript. However, our works present a distinct comprehension on structure-spectral shift relationship for gas phase fluorescent protein chromophores. It is undoubtedly helpful to fluorescent protein red shift mutant designing of experiment.

Acknowledgments. The author would like to thank research initiation fund of HTU and key fund of HeNan province education department (14A140031).

References

[1] D. C. Prasher, V. K. Eckenrode, W. W. Ward, *et al.* Gene. 111(2) (1992) 229.
[2] M. OrmÖ, A. B. Cubitt, K. Kallio, *et al.* Science. 273(5280) (1996) 1392.
[3] C Guthrie, G Fink and Eds. Anal. Biochem. 315(2) (2003) 289.
[4] R N. Day and M W. Davidson. Chem. Soc. Rev. 38(10) (2009) 2887.
[5] M. Chale, Y. Tu and G. Euskirchen, *et al.* Science. 263(5148) (1994) 802.
[6] B. N. Giepmans, S. R. Adams, M. H. Ellisman, *et al.* Science. 312(5771) (2006) 217.
[7] J. Lippincott-Schwartz and G. H. Patterson. Science. 300(5616) (2003) 87.
[8] R. Heim, D. C. Prasher and R. Y. Tsien. Pro. Natl. Acad. Sci. U S A. 91(26) (1994) 12501.
[9] S. J. Davis and R. D. Vierstra. Plant. Mol. Biol. 36(4) (1998) 521.
[10] T. T. Yang, P. Sinai and G. Green, *et al.* J. Biol. Chem. 273(14) (1998) 8212.
[11] M. A. Rizzo, G. H. Springer ,B. Granada, *et al.* Nat.Biotechnol. 22(4) (2004) 445.
[12] N. C. Shaner, R. E. Campbell, P. A. Steinbach, *et al.* Nat. biotechnol. 22(12) (2004) 1567.
[13] T. Nagai, K. Ibata, E. S. Park, *et al.* Nat. biotechnol. 20(1) (2002) 87.
[14] R. E. Campbell, O. Tour, A. E. Palmer, *et al.* Pro. Natl. Acad. Sci. U S A/Pnas. 99(12) (2002) 7877.
[15] AC. Stiel, M. Andresen, H. Bock, *et al.* Biophys. J. 95(6) (2008) 2989.
[16] T. Kukar, S. Eckenrode, Y. Gu, *et al.* Anal. Biochem. 306(1) (2002) 50.
[17] PI. H. Bastiaens and R. Pepperkok. Trends .Biochem. Sci. 25(12) (2000) 631.
[18] Y. Osamura, W T. Borden and K Morokuma. J. Am. Chem. Soc/Jacs. 106(18) (1984) pp 5112.
[19] J. Full, L. Gonzalez and C. Daniel. J. Phys. Chem. A. 105(1) (2001) 184.
[20] M N. Glukhovtsev, R D. Bach and C J. Nagel. J. Phys. Chem. A. 101(3) (1997) pp 316.
[21] T. Yanaia, D P. Tewb and N C. Handyb. Chem. Phys. Lett. 393(1) (2004) 51.
[22] K A. Nguyen, P N. Day and R. Pachter. Int. J. Quantum .Chem. 110(12) (2010) 2247.
[23] C. Filippi , F. Buda, L. Guidoni, *et al.* J. Chem. Theory .Comput. 8(1) (2012) pp 112.

[24] X. Liu, J. Li, C. Hu, *et al.* Angew. Chem. -Int. Edit. 52(18) (2013) 4805.
[25] P. Amat and R. Nifosi . J. Chem. Theory .Comput. 9 (2013) 497.
[26] X. Li, L. W. Chung, H. Mizuno. *et al.* Chem. B. 114(2) (2010) 1114.
[27] G. Zhao, K. Han, J. Chem. Comput. 29(12) (2008) 2010.
[28] R. J Cave, E. W. Castner. J. Phys. Chem. A. 106(50) (2002) 12117.